

Generic mechanism for generating a liquid-liquid phase transition.

Giancarlo Franzese¹, Gianpietro Malescio², Anna Skibinsky¹, Sergey V. Buldyrev¹, and H. Eugene Stanley¹

¹Center for Polymer Studies and Department of Physics, Boston Univ., Boston, MA 02215, USA

²Dipartimento di Fisica, Università di Messina and Istituto Nazionale Fisica della Materia, 98166 Messina, Italy

(October 29, 2018)

Recent experimental results [1] indicate that phosphorus, a single-component system, can have two liquid phases: a high-density liquid (HDL) and a low-density liquid (LDL) phase. A first-order transition between two liquids of different densities [2] is consistent with experimental data for a variety of materials [3,4], including single-component systems such as water [5–8], silica [9] and carbon [10]. Molecular dynamics simulations of very specific models for supercooled water [2,11], liquid carbon [12] and supercooled silica [13], predict a LDL-HDL critical point, but a coherent and general interpretation of the LDL-HDL transition is lacking. Here we show that the presence of a LDL and a HDL can be directly related to an interaction potential with an attractive part and two characteristic short-range repulsive distances. This kind of interaction is common to other single-component materials in the liquid state (in particular liquid metals [14–21,2]), and such potentials are often used to describe systems that exhibit a density anomaly [2]. However, our results show that the LDL and HDL phases can occur in systems with no density anomaly. Our results therefore present an experimental challenge to uncover a liquid-liquid transition in systems like liquid metals, regardless of the presence of the density anomaly.

Several explanations have been developed to understand the liquid-liquid phase transition. For example, the *two-liquid models* [4] assume that liquids at high pressure are a mixture of two liquid phases whose relative concentration depends on external parameters. Other explanations for the liquid-liquid phase transition assume an anisotropic potential [2,11–13]. Here we shall see that liquid-liquid phase transition phenomena can arise solely from an isotropic pair interaction potential with two characteristic lengths.

For molecular liquid phosphorus P_4 (as for water), a tetrahedral open structure is preferred at low pressures P and low temperatures T , while a denser structure is favored at high P and high T [1,6,8]. The existence of these two structures with different densities suggests a pair interaction with two characteristic distances. The first distance can be associated with the *hard-core* exclusion between two particles and the second distance with a weak repulsion (*soft-core*), which can be overcome at large pressure. Here we will use a generic three dimensional (3D) model composed of particles interacting via

an isotropic soft-core pair potential. Such isotropic potentials can be regarded as resulting from an average over the angular part of more realistic potentials, and are often used as a first approximation to understand the qualitative behavior of real systems [14–22,2]. For Ce and Cs, Stell and Hemmer proposed a potential with nearest-neighbor repulsion and a weak long-range attraction [15]. By means of an exact analysis in 1D, they found two critical points, with the high-density critical point interpreted as a solid-solid transition. Then analytic calculations [16], simulations [17] and exact solution in 1D [18] of the structure factor for a model with a soft-core potential were found consistent with experimental structure factors for liquid metals such as Bi. The structure factor was also the focus of a theoretical study of a family of soft-core potentials, for liquid metals, by means of mean-spherical approximation [19]. More recently, the analysis of the solid phase of a model with a soft-core potential [20] was related to the experimental evidence of a liquid-liquid critical point in the K_2Cs metallic alloy [21]. Moreover, for simple metals, soft-core potentials have been derived by first-principle calculations [14] and computed from experimental data [2]. The importance of soft-core potentials in the context of supercooled liquids was pointed out by Debenedetti and others [23–25], and the analysis of experimental data for water gives rise to a soft-core potential [26].

The isotropic pair potential considered here (Fig.1a, inset) has a hard-core radius a and a soft-core radius $b > a$. For $a < r < b$ the particles repel each other with energy $U_R > 0$, for $b < r < c$ they attract each other with energy $-U_A < 0$. For $r > c$ the interaction is considered negligible and is approximated to zero. The potential has three free parameters: b/a , c/a and U_R/U_A .

To select the parameters for the molecular dynamics (MD) simulations is not easy, and MD is too time consuming to study a wide range of parameter values. Hence we first perform an integral equation analysis [27], whose predictions we can calculate very rapidly and efficiently. In this technique, one derives the phase diagram by studying the static pair distribution function – which measures the probability of finding a particle at a given distance from a reference particle, and thereby quantifies the correlation between pairs of particles. Mathematically, this function can be written as the sum of an infinite series of many-dimensional integrals, over particle coordinates, involving the pair interaction potential. Since this exact expression is intractable, approximations must be made. Here we use the hypernetted-chain ap-

proximation, which consists of neglecting a specific class of these integrals, leading to a simplified integral equation that can be solved numerically. In the temperature - density (T - ρ) phase diagram, the region where the simplified equation has no solutions is related [27] to the region where the system separates in two fluid phases. Thus this technique allows us to estimate the parameter range where two critical points occur, and hence to find useful parameters values for the MD simulations: $b/a = 2.0$, $c/a = 2.2$ and $U_R/U_A = 0.5$. We also use in the MD calculations several additional parameter sets.

Specifically we perform MD simulations in 3D at constant volume V and number of particles $N = 490$ and 850. We use periodic boundary conditions, a standard collision event list algorithm [24], and a modified Berendsen method to control T [28]. We find, for each set of parameters, the appearance of two critical points (Fig.1).

A critical point is revealed by the presence of a region, in the P - ρ phase diagram, with negative-slope isotherms. In MD simulations this region is related to the coexistence of two phases [2]. The (local) maximum and minimum along an isotherm correspond to the limits of stability of the existence of each single phase (supercooled and superheated phase, respectively). By definition, these maxima and minima are points on the *spinodal line* for that temperature. Since the spinodal line has a maximum at a critical point, a way to locate a critical point is to find this maximum. In our simulations (Fig.1), we find two regions with negatively-sloped isotherms and the overall shape of the spinodal line has two maxima, showing the presence of *two* critical points, C_1 and C_2 . Using the Maxwell construction in the P - V plane [2], we evaluate the *coexistence lines* of the two fluid phases associated with each critical point (Fig.2). Considering both the maxima of the spinodal line and the maxima of the coexistence regions in the P - ρ and P - T planes, we estimate the low-density critical point C_1 at $T_1 = 0.606 \pm 0.004 U_A/k_B$, $P_1 = 0.0177 \pm 0.0008 U_A/a^3$, $\rho_1 = 0.11 \pm 0.01 a^{-3}$ and the high-density critical point C_2 at $T_2 = 0.665 \pm 0.005 U_A/k_B$, $P_2 = 0.10 \pm 0.01 U_A/a^3$, $\rho_2 = 0.32 \pm 0.03 a^{-3}$. Critical point C_1 is at the end of the phase transition line separating the gas phase and the LDL phase, while critical point C_2 is at the end of the phase transition line separating the gas phase and the HDL phase. Their relative positions resemble the phosphorus phase diagram, except that, in the experiments, C_2 has not been located [1], but is expected at the end of the gas-HDL transition line.

Our phase diagram (Fig.2) shows the following fluid phases. At high $T > T_2$, the only fluid phase is the gas. At $T_1 < T < T_2$, we find - depending on ρ - the gas alone, or the HDL alone (turquoise region), or the HDL coexisting with gas (black line in Fig.2a and green region in Fig.2c). Below T_1 , the LDL phase appears alone (blue region), or in coexistence with the HDL (orange line in Fig.2b and orange region in Fig.2d), or in coexis-

tence with the gas (red line in Fig.2b and red region in Fig.2d). The point where the gas-LDL coexistence line merges with the LDL-HDL coexistence line is the *triple point*. Below the pressure and temperature of the triple point, LDL is not stable and separates into gas and HDL.

For phosphorus the liquid-liquid transition occurs in the stable fluid regime [1]. In contrast, for our model, it occurs in the metastable fluid regime (see Fig.1). We therefore wish to understand how to enhance the stability of the critical points with respect to the crystal phase. We find that by increasing the attractive well width $(c-b)/a$, both critical temperatures T_1 and T_2 increase, and hence both critical points move toward the stable fluid phase, analogous to results for attractive potentials with a single critical point [29,30]. For example, for attractive well width $(c-b)/a = 0.2$, both C_1 and C_2 are *metastable* with respect to the crystal, while for $(c-b)/a > 0.7$ we find C_1 in the *stable* fluid phase.

The phase diagram depends sensitively also on the relative width of the shoulder b/a and on its relative height U_R/U_A . By decreasing b/a or by increasing U_R/U_A , T_2 decreases and becomes smaller than T_1 . This means that, in these cases, the high-density C_2 occurs below the temperature of the gas-liquid critical point, i.e. C_2 is in the liquid phase and represents a LDL-HDL critical point, as in supercooled water [6,7,11].

The soft-core potential with the sets of parameter we use displays no "density anomaly" $(\partial V/\partial T)_P < 0$. This result is at first sight surprising since soft-core potentials have often been used to explain the density anomaly (see, e.g., Refs. [2,24]). To understand this result, we consider the entropy S (the degree of disorder in the system) and the thermodynamic relation $-(\partial V/\partial T)_P = (\partial S/\partial P)_T = (\partial S/\partial V)_T(\partial V/\partial P)_T$. Since of necessity $(\partial V/\partial P)_T < 0$, $(\partial V/\partial T)_P < 0$ implies $(\partial S/\partial V)_T < 0$, i.e. the density anomaly implies that the disorder in the system increases for decreasing volume. For example, this is the case for water. This is consistent with the negative slope dP/dT of the crystal-liquid transition line for water, that implies $\Delta S/\Delta V < 0$ for the Clausius-Clapeyron equation $dP/dT = \Delta S/\Delta V$, where ΔS and ΔV are the entropy and volume differences between the two coexisting phases.

For our system, we expect the reverse: $(\partial V/\partial T)_P > 0$ so $(\partial S/\partial V)_T > 0$, consistent with the positive slope of the LDL-HDL transition line dP/dT (see Fig.2b). We confirm our expectation that $(\partial S/\partial V)_T > 0$ by explicitly calculating S for our system by means of thermodynamic integration.

Our results show that the presence of two critical points and the occurrence of the density anomaly are not necessarily related, suggesting that one might seek experimental evidence of a liquid-liquid phase transition in systems with no density anomaly. In particular, a second critical point may also exist in liquid metals that can be described by soft-core potentials. Thus the class

of experimental systems displaying a second critical point may be broader than previously hypothesized.

-
- [1] Katayama, Y., Mizutani, T., Utsumi, W., Shimomura, O., Yamakata, M., & Funakoshi, K. A first-order liquid-liquid phase transition in phosphorus. *Nature* **403**, 170–173 (2000).
- [2] Debenedetti, P.G. *Metastable Liquids: Concepts and Principles* (Princeton Univ. Press, Princeton, 1998).
- [3] Wilding, M. C., McMillan, P. F., & Navrotsky A. The thermodynamic nature of a phase transition in yttria-alumina liquids. *J. Noncryst. Solids* (in the press).
- [4] Brazhkin, V. V., Popova, S. V. & Voloshin, R. N. High-pressure transformations in simple melts. *High Pressure Res.* **15**, 267–305 (1997).
- [5] Brazhkin, V. V., Gromnitskaya, E. L., Stalgorova, O. V. & Lyapin, A. G. Elastic softening of amorphous H₂O network prior to the HDA-LDA transition in amorphous state. *Rev. High Pressure Sci. Tech.* **7**, 1129–1131 (1998).
- [6] Mishima, O. Liquid-liquid critical point in heavy water. *Phys. Rev. Lett.* **85**, 334–336 (2000).
- [7] Bellissent-Funel, M.-C. Evidence of a possible liquid-liquid phase transition in supercooled water by neutron diffraction. *Nuovo Cimento* **20D**, 2107–2122 (1998).
- [8] Soper, A. K. & Ricci, M. A. Structures of high-density and low-density water. *Phys. Rev. Lett.* **84**, 2881–2884 (2000).
- [9] Lacks, D. J. First-order amorphous-amorphous transformation in silica. *Phys. Rev. Lett.* **84**, 4629–4632 (2000).
- [10] van Thiel M. & Ree F. H. High-pressure liquid-liquid phase change in carbon. *Phys. Rev. B* **48**, 3591–3599 (1993).
- [11] Poole, P. H., Sciortino, F., Essmann, U., & Stanley, H. E. Phase behavior of metastable water. *Nature* **360**, 324–328 (1992).
- [12] Glosli, J. N. & Ree, F. H. Liquid-Liquid Phase Transformation in Carbon. *Phys. Rev. Lett.* **82**, 4659–4662 (1999).
- [13] Saika-Voivod I., Sciortino F. & Poole P. H. Computer simulations of liquid silica: Equation of state and liquid-liquid phase transition. *Phys. Rev. E* **63**, vol. 1 (2000) (in press).
- [14] Mon, K. K., Ashcroft, M. W. & Chester, G. V. Core polarization and the structure of simple metals. *Phys. Rev. B* **19**, 5103–5118 (1979).
- [15] Stell, G. & Hemmer, P.C. Phase transition due to softness of the potential core. *J. Chem. Phys.* **56**, 4274–4286 (1972).
- [16] Silbert, M. & Young, W.H., Liquid metals with structure factor shoulders. *Phys. Lett.* **58A**, 469–470 (1976).
- [17] Levesque, D. & Weis, J.J., Structure factor of a system with shouldered hard sphere potential. *Phys. Lett.* **60A**, 473–474 (1977).
- [18] Kincaid, J.M. & Stell, G. Structure factor of a one-dimensional shouldered hard-sphere fluid. *Phys. Lett.* **65A**, 131–134 (1978).
- [19] Cummings, P.T. & Stell, G. Mean spherical approximation for a model liquid metal potential. *Mol. Phys.* **43**, 1267–1291 (1981).
- [20] Velasco, E., Mederos, L., Navascués, G., Hemmer, P.C., & Stell, G. Complex phase behavior induced by repulsive interactions. *Phys. Rev. Lett.* **85**, 122–125 (2000).
- [21] Voronel, A., Paperno, I., Rabinovich, S., & Lapina, E. New critical point at the vicinity of freezing temperature of K₂Cs. *Phys. Rev. Lett.* **50**, 247–249 (1983).
- [22] Behrens, S. H., Christl, D. I., Emmerzael, R., Schurtenberger, P., & Borkovec, M. Charging and aggregation properties of carboxyl latex particles: Experiments versus DLVO theory. *Langmuir* **16**, 2566–2575 (2000).
- [23] Debenedetti, P. G., Raghavan, V. S. & Borick, S. S. Spinodal curve of some supercooled liquids. *J. Phys. Chem.* **95**, 4540–4551 (1991).
- [24] Sadr-Lahijany, M.R., Scala, A., Buldyrev, S.V., & Stanley, H. E. Liquid state anomalies for the Stell-Hemmer core-softened potential. *Phys. Rev. Lett.* **81**, 4895–4898 (1998).
- [25] Jagla, E. A. Core-softened potentials and the anomalous properties of water. *J. Chem. Phys.* **111**, 8980–8986 (1999).
- [26] Stillinger, F. H. & Head-Gordon, T. Perturbational view of inherent structures in water. *Phys. Rev. E* **47**, 2484–2490 (1993).
- [27] Caccamo, C. Integral equation theory description of phase equilibria in classical fluids. *Phys. Rep.* **274**, 1–105 (1996).
- [28] Berendsen, H. J. C., Postma, J. P. M., van Gunsteren, W. F., DiNola, A. & Haak, J. R. Molecular dynamics with coupling to an external bath. *J. Chem. Phys.* **81**, 3684–3690 (1984).
- [29] Rein ten Wolde, P. & Frenkel, D. Enhancement of protein crystal nucleation by critical density fluctuations. *Science* **277**, 1975–1978 (1997).
- [30] Hagen, M. H. J., Meijer, E. J., Mooij, G. C. A. M., Frenkel, D., Lekkerkerker, H. N. W. Does C-60 have a liquid-phase? *Nature* **365**, 425–426 (1993).

Acknowledgments

We wish to thank L.A.N. Amaral, P.V. Giaquinta, E. La Nave, T. Lopez Ciudad, S. Mossa, G. Pellicane, A. Scala, F.W. Starr, J. Teixeira, and, in particular, F. Sciortino and two anonymous referees for helpful suggestions and discussions. We thank NSF and CNR (Italy) for partial support.

FIG. 1. Pressure-density isotherms, crystallization line and spinodal line from the MD simulations for the isotropic pair potential in 3D. **(a), Inset:** The pair potential energy $U(r)$ as a function of the distance r between two particles. **(a)** Several isotherms for (bottom to top) $k_B T/U_A = 0.57, 0.59, 0.61, 0.63, 0.65, 0.67$ (k_B is the Boltzmann constant). Diamonds represent data points and lines are guides for the eyes. The solid line connecting local maxima and minima along the isotherms represents the *spinodal line*. The two maxima of the spinodal line (squares) represent the two critical points C_1 and C_2 . To determine the *crystallization line* (gray line) – below which the fluid is metastable with respect to the crystal – we place a crystal seed, prepared at very low T , in contact with the fluid, and check, for each (T, ρ) , if the seed grows or melts after 10^6 MD steps. The spontaneous formation (*nucleation*) of the crystal is observed, within our simulation times ($\approx 10^5$ MD steps), only for $\rho \geq 0.27 a^{-3}$. We use the structure factor $S(Q)$ – the Fourier transform of the density-density correlation function for wave vectors Q – to determine when the nucleation occurs. Indeed, at the onset of nucleation, $S(Q)$ develops large peaks at finite Q ($Q = 12a^{-1}$ and $Q = 6a^{-1}$). For each ρ , we quench the system from a high- T configuration. After a transient time for the fluid equilibration, we compute $P(T, \rho)$, averaging over $10^5 - 10^6$ configurations generated from up to 12 independent quenches, making sure that the calculations are done before nucleation takes place. **(b)** Enlarged view of the region around the gas-LDL critical point C_1 for $k_B T/U_A = 0.570, 0.580, 0.590, 0.595, 0.600, 0.610, 0.620, 0.630$.

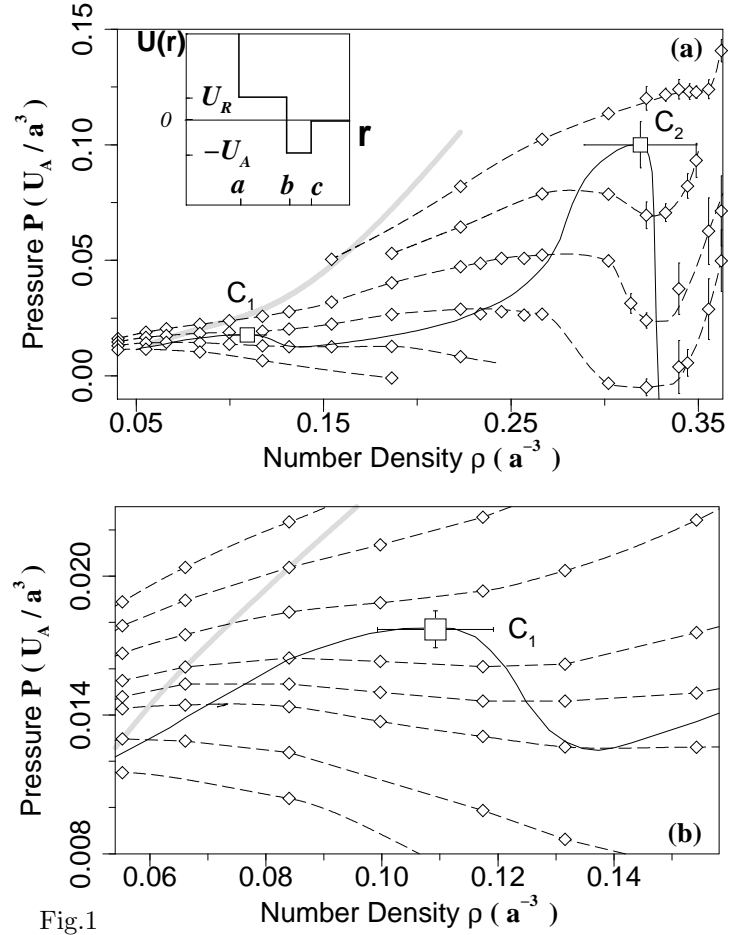


Fig.1

FIG. 2. The phase diagrams, with coexistence lines and critical points resulting from MD simulations. **(a,b)** P - T phase diagram. Panel (b) is a blow up of panel (a) in the vicinity of C_1 . Circles represent points on the coexistence lines: open circles are for the gas-LDL coexistence, filled circles for the gas-HDL coexistence. Lines are guides for the eyes. The solid black line is the gas-HDL coexistence line. The red line is the gas-LDL coexistence line. The solid red line is stable, while the dashed red line is metastable, with respect to the HDL phase. The orange line is the LDL-HDL coexistence line. The triangle represents the *triple point*. The projection of the spinodal line is represented in (a) and (b) by diamonds with dashed lines. The spinodal line is folded in this projection, with two cusps corresponding to the two maxima in Fig.1. Critical points occur where the coexistence lines meet these cusps. The critical point C_1 is for the gas-LDL transition, and C_2 is for the gas-HDL transition. **(c,d)** P - ρ projections of panels (a,b). The colors, symbols and patterns of coexistence lines, triple and critical points are the same as in panel (a,b). Dashed blue, black and orange lines schematically represent isotherms at the temperatures of C_1 , C_2 and of the triple point, respectively. Both gas-LDL and gas-HDL coexistence lines show a local maximum, representing the estimates of C_1 and C_2 , respectively. In all the panels, where not shown, the errors are smaller than the symbol size.

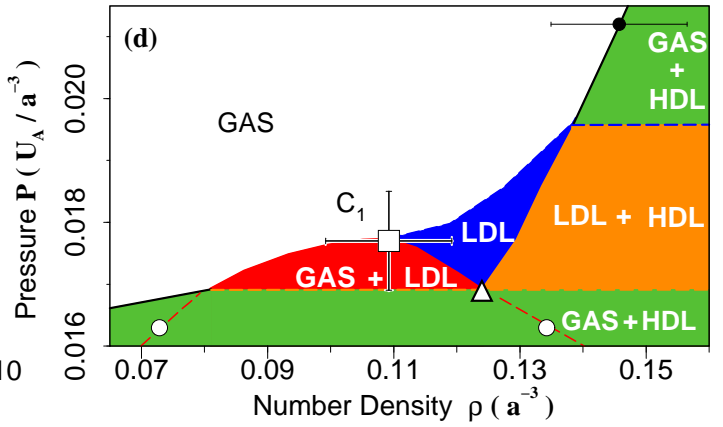
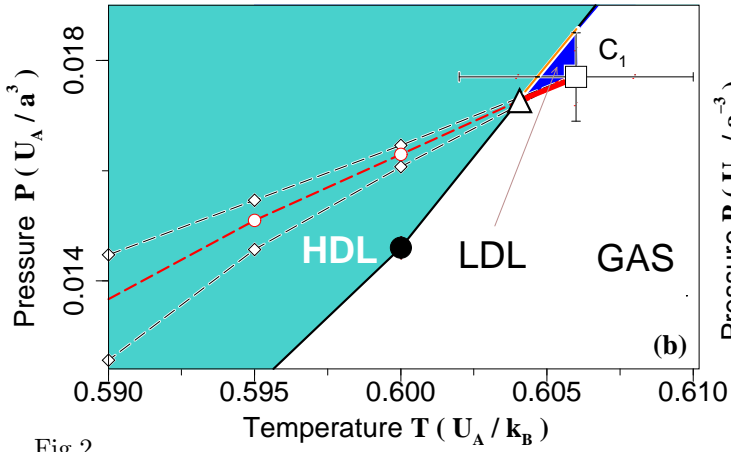
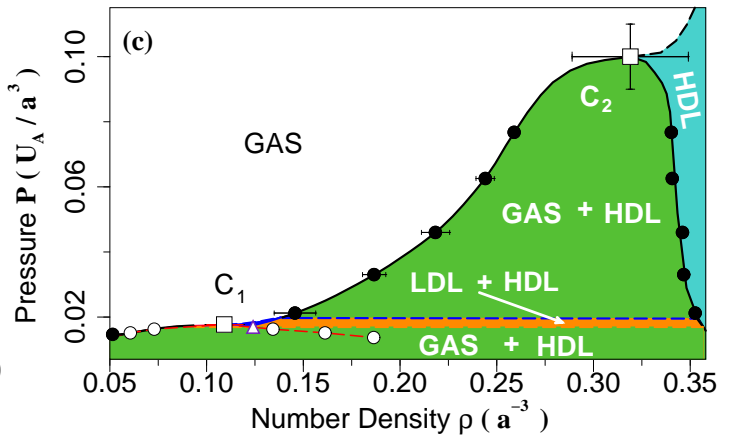
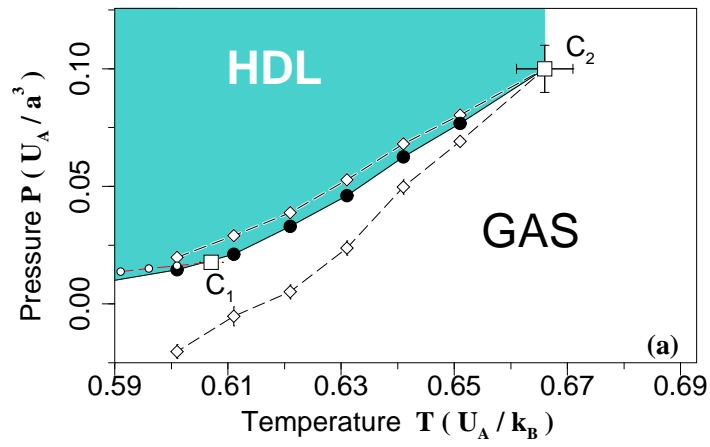


Fig.2